Proceedings of the 2000 DOE Hydrogen Program Review
NREL/CP-570-28890

THERMAL DISSOCIATION OF METHANE USING A SOLAR COUPLED AEROSOL FLOW REACTOR

Alan W. Weimer, Jaimee Dahl, and Joseph Tamburini
University of Colorado, Department of Chemical Engineering
Boulder, CO 80309-0424

Allan Lewandowski, Roland Pitts, and Carl Bingham
National Renewable Energy Laboratory
Golden, CO 80401-3393

Gregory C. Glatzmaier
Peak Design
Evergreen, CO 80439

Abstract

A solar-thermal aerosol flow reactor has been constructed, installed and tested at the High-Flux Solar Furnace (HFSF) at the National Renewable Energy Laboratory (NREL). "Proof-of-concept" experiments were successfully carried out for the dissociation of methane to produce hydrogen and carbon black. Approximately 90% dissociation of methane was achieved in a 25-mm diameter quartz reaction tube illuminated with a solar flux of 2400 kW/m^2 (or suns). Preliminary economics for a 1,000,000 kg/yr solar-thermal hydrogen plant were evaluated using a discount cash flow analysis that required a 15% Internal Rate of Return (IRR). If either product is the sole source of revenue, the required selling price for hydrogen was $27/MBtu ($0.092/kWhr or $25.6/GJ) and for carbon black it was $0.55/lb ($1.21/kg). If both products are sold, and carbon black is sold for $0.35/lb ($0.77/kg), the required selling price for hydrogen was $10/MBtu ($9.47/GJ or $0.034/kWhr). Both the experimental and economic results are very encouraging and support further work to address the technical issues and to develop the process.

Introduction

The primary driver for the development of renewable energy strategies is current concern over the potential, irreversible environmental damage that may occur with the continued or accelerated use of fossil fuels. Movement toward a hydrogen (H_2) based economy is an essential component of an international program to address that concern and will, in addition, address concerns over pollution in cities and associated health costs. However, current methods for producing H_2 incur a large environmental liability because fossil fuels are burned to supply the energy to reform methane (CH_4). We propose an alternate strategy using highly concentrated sunlight as the energy source that does not result in an increase of environmental liability. Indeed, it represents a route for utilizing current natural gas reserves that fixes carbon as well as increasing the energy content of the fuel. The research presented here is oriented at developing a cost-effective, solar-thermal method of deriving H_2 from natural gas.

Background

Steinberg [1986, 1987, 1994, 1995, 1998, 1999] and Steinberg and co-workers [Steinberg and Cheng, 1989] have been major proponents of the thermal decomposition of CH_4 process for H_2 production. Methane (CH_4) is dissociated to carbon (C) black and H_2 according to:

$$CH_4 \rightarrow C + 2H_2 \qquad \Delta H_{298K} = 74.9 \text{ kJ/mol} \qquad (1)$$

Methane (CH_4) is a preferred choice for the production of H_2 from a hydrocarbon because of its high H to C ratio (H/C = 4), availability, and low cost. Furthermore, the C produced can be sold as a co-product into the carbon black market (inks, paints, tires, batteries, etc.) or sequestered, stored, and used as a clean fuel for electrical power generation. The sequestering or storing of solid C requires much less development than sequestering gaseous CO_2.

Gibbs free energy minimization calculations have been carried out (P = 0.1 MPa; $873 \text{ K} \leq T \leq 2273 \text{ K}$) for the CH_4 dissociation system (i.e. CH_4 + heat ➔ equilibrium products) to determine equilibrium products. The concentrations of chemical species reaching a state of chemical equilibrium from reaction or partial reaction at atmospheric pressure for various reaction temperatures have been calculated using the F*A*C*T equilibrium code EQUILIB (Thompson et al., 1985]. Thermodynamically favored products (Figure 1) indicate dissociation above 600 K and that temperatures T > 1600 K are required to achieve nearly complete dissociation. Although not shown, trace products at 1600 K include C_2H_2, C_2H_4, C_4H_8, C_3H_6, C_2H_6, and other species at concentrations < 40 ppm.

There are several alternatives to supply the energy required to drive reaction (1). In the commercial “Thermal Black Process” [Donnet, 1976], the energy is provided by burning CH_4 with air to heat a fire brick furnace to temperatures as high as 1673 K. Once hot, the air is shut off and the CH_4 decomposes according to reaction (1) until the wall temperature drops to below 1073 K. The system is operated semi-continuously with CH_4 burned in one sequence of the cycle to supply the heat necessary to carry out the decomposition in the second sequence. This process has been practiced for many years for the production of carbon black. The H_2 produced is used as a fuel to heat the furnace and the CH_4 feedstock.

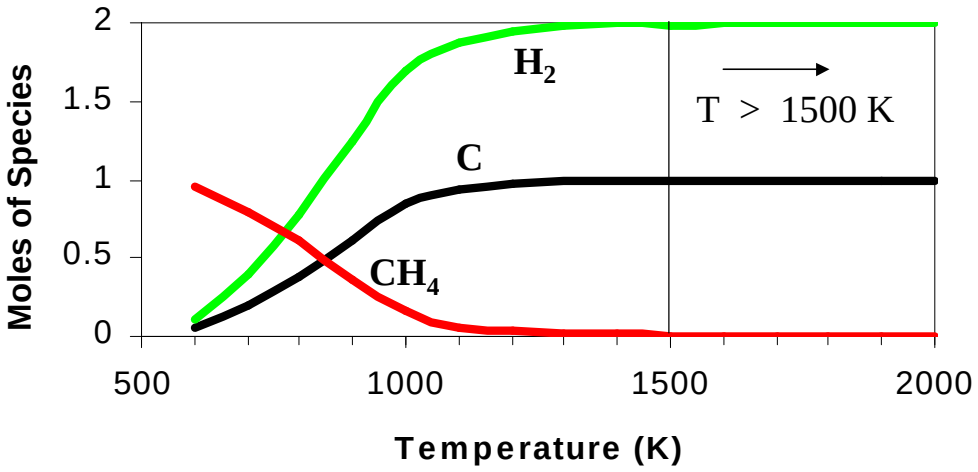

Figure 1. Primary Methane Decomposition Equilibrium Products P = 0.1 MPa

Pohleny and Scott (1962) used a fluidized bed/riser thermal decomposition reactor process that uses iron oxide for heat transfer and as a catalyst. Carbon collected on the iron oxide particles in the fluidized bed is burned off in the riser reactor for reheating the iron oxide particles that are recirculated to the endothermic fluidized bed reactor. Hydrogen is produced continuously by the decomposition occurring in the fluidized bed.

Gaudermack and Lynum (1996) and Bromberg et al. (1998) used a plasma torch to supply the necessary energy to decompose CH_4 and produce a continuous stream of H_2. The plasma gas is H_2 that is recirculated from the process. Although no CO_2 is liberated from the process reactor itself, electricity is required to produce the plasma. When the electrical power is produced from natural gas fuel combustion, even in an efficient combined cycle plant, the overall thermal efficiency is significantly reduced and the CO_2 emission per unit energy is significantly increased.

In another process [Steinberg, 1995a], a molten metal bath reactor (such as tin or copper) is used to transfer heat to CH_4 that is bubbled through the molten metal. The reactor is heated by combustion products (CH_4 or H_2 burned with air) that flow through an internal heat exchanger. In this process, it is proposed to capture carbon in the liquid metal and to separate it from the metal by density difference, skimming the carbon off from the surface much as slag is skimmed off the surface of molten iron in a conventional blast furnace.

Although thermodynamics can predict when a reaction will not occur, it cannot predict whether a reaction will indeed occur in practice. Activation energies, transport processes (e.g. heating rate), and other reaction kinetic considerations are needed in order to determine if a reaction can be completed for a given amount of time in a chemical reactor design. Such kinetic data have been reported for reaction (1) using electrically heated pilot-scale aerosol flow reactors [Matovich, 1977].

Matovich (1977) showed that the decomposition of CH_4 could be carried to completion in a short residence time aerosol reaction tube at temperatures T > 2088 K. The reactor consisted of a 0.0762-m diameter x 0.914-m long (3 inch ID x 3 ft long) graphite aerosol reaction tube heated indirectly by radiation from external electrodes heated directly by electrical resistance. Later studies included work carried out in 0.305-m ID x 3.66-m long (1 ft ID x 12 ft long) reaction tubes [Lee et al., 1984]. A small amount of carbon black was introduced in the CH_4 feed stream to serve as a radiation-absorbing target to initiate the pyrolytic reaction. Due to the high temperatures involved and the difficulty in heating a gas to those temperatures (by convection from the reactor walls), the carbon particles are the key to this process.

Reactions were carried out in the temperature range of 1533 < T < 2144 K with residence times between approximately 0.1 and 1.5 seconds. The fraction of CH_4 dissociated was determined by measuring the thermal conductivity of the effluent gas after filtering the carbon black particles from the sample. Hydrogen (H_2) flowed radially through a porous reaction tube, providing a fluid-wall to prevent carbon black from depositing on the wall. The residence time in the reactor was controlled by the inlet flow of CH_4, the radial flow of H_2, and the reactor temperature. Some reported results [Matovich, 1977] where data were available for both a minimum residence time ($t_{r(min)}$) of 0.2 s and a maximum residence time ($t_{r(max)}$) of 1 s are summarized in Figure 2. It is clear from these results that residence time has little effect on dissociation for temperatures T > 1900 K and that complete dissociation can be achieved in aerosol flow reactors for temperatures greater than approximately 2100 K for reaction times of t = 0.2 s.

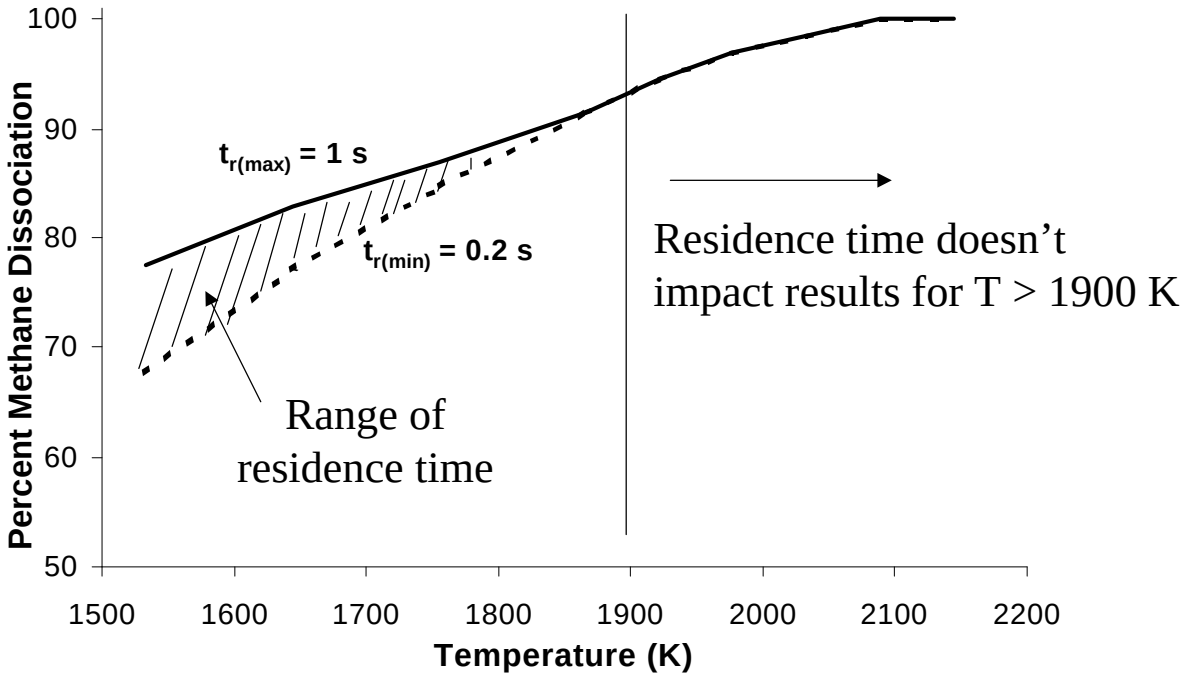

Figure 2. Effect of Residence Time & Temperature

The process investigated here is the high-temperature thermal dissociation of CH_4 using a solar-thermal aerosol flow reactor. The energy required to drive reaction (1) is supplied by concentrated sunlight. An experimental reactor apparatus was constructed and interfaced to NREL's HFSF [Jenkins et al., 1996; Lewandowski, 1993; Lewandowski et al., 1991; and Pitts et al., 1993]. There is no need for auxiliary cooling at the optical source. The reactor is operated as a cold wall process, because the beam is delivered directly on target. In addition, the control of solar radiation (on/off) is almost instantaneous. Absorbing surfaces exposed to concentrated solar radiation can reach temperatures of between 1000 K and 3000 K in fractions of a second. The process produces H_2 using high efficiency direct solar-thermal heating with no associated CO_2 generation.

Experimental Work

High-Flux Solar Furnace

The HFSF facility (Figure 3) at NREL in Golden, CO was used for this research. NREL is the primary national laboratory in the United States for renewable energy research. The HFSF uses a series of mirrors that concentrate sunlight to a focused beam at maximum power levels of 10 kW into an approximate diameter of 10 cm. The solar furnace's long focal length and its off-axis design give researchers flexibility and control over the delivered flux. It operates with a heliostat that has an area of 31.8 m^2 and a 92% solar-weighted reflectivity. The heliostat reflects sunlight to a primary concentrator consisting of 25 hexagonal facets that are spherical mirrors ground to a 14.6-m radius of curvature. The total surface area of the primary concentrator is 12.5 m^2 and it reflects radiation from the entire solar spectrum (300 nm to 2500 nm). Under optimal conditions, the primary concentrator can achieve maximum flux intensities of 2,500 suns. Secondary concentrators that achieve intensities of more than 20,000 suns and refractive designs approaching 50,000 suns can be installed at the primary concentrator's focal point to increase the intensity further. The furnace is easily capable of delivering flux densities on the order of 100-1000 W/cm^2. No secondary solar concentration was used in these studies.

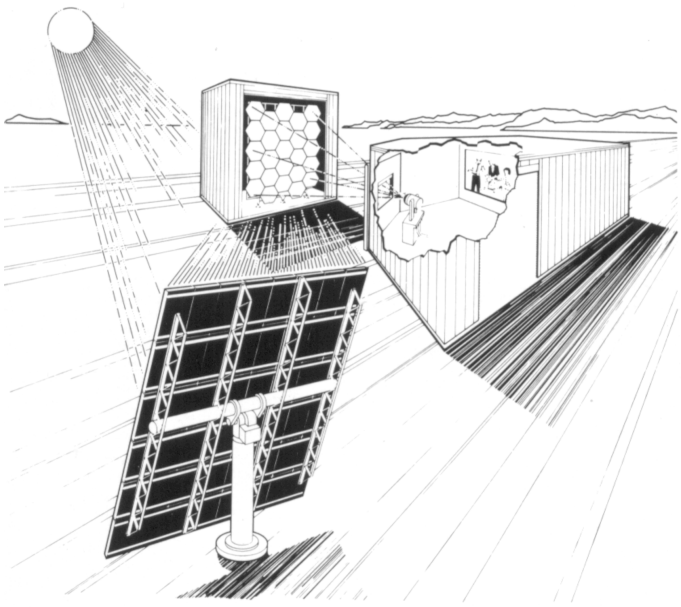

Figure 3. High-Flux Solar Furnace Schematic

Reactor System

Proof-of-concept experiments were carried out using a modified reactor system originally built for previous experiments in fullerene production [Mischler et al., 1997]. The reactor consists of a particle and gas feed mechanism, quartz reactor tube, an internal graphite "target" feed tube, and a filter housing. The reactor operates at atmospheric pressure with gas flow driven and controlled through a series of mass flow controllers. An in-line Horiba model TCA-300 H_2 detector was inserted downstream of the particle filter. This detector is based on thermal conductivity measurements and was calibrated for 5 % H_2 in argon (Ar). Gas samples were also taken and analyzed using an off-line gas chromatograph (GC). CH_4 and produced H_2 were kept outside flammability limits by operating with a dilute 5% CH_4 in Ar feed gas mixture and a pure Ar purge stream. The temperature inside the quartz tube reactor is exceedingly difficult to determine. However, the temperature of the quartz tube is carefully monitored using an infrared camera positioned on the side of the reactor. The quartz temperature is monitored to avoid warping or even melting the reactor wall with concentrated sunlight. A schematic of the reactor system is shown in Figure 4.

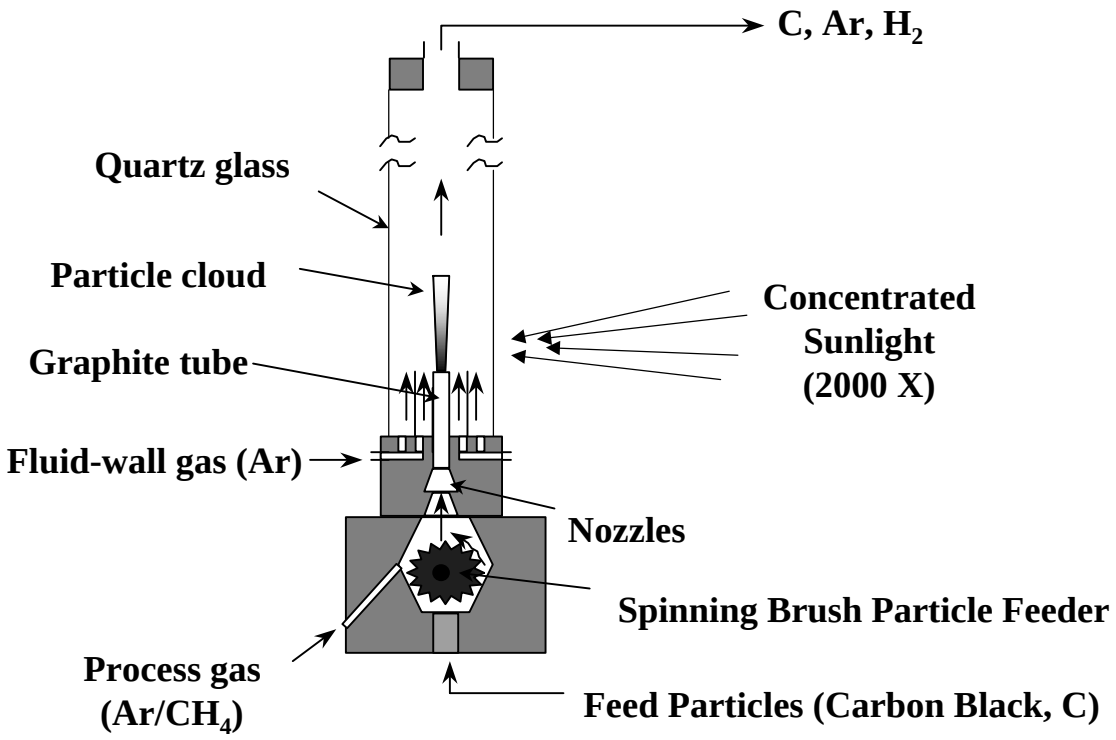

Figure 4. Schematic of Solar-thermal Aerosol Flow Reactor

A key aspect of the reactor operation is the heating means for the feed CH_4. The reactor has been designed for three alternative heating methods: (1) heating a 6 mm OD x 3 mm thick "target" graphite tube with concentrated sunlight, the heated target then heating the CH_4-containing feed gas by conduction; (2) heating the "target" graphite tube, but with radiation absorbing fine carbon black particles suspended in the CH_4-containing feed gas stream so the inside wall of the

"target" radiates to the flowing particles that subsequently heat the flowing feed gas by particle surface conduction in addition to the wall conduction; and (3) heating the suspended carbon black particles directly with concentrated sunlight, the sunlight directed above the top of the graphite tube. Alternatives (2) and (3) involve volumetric absorption of light by a gas-solid suspension. The graphite tube can be seen contained within the quartz tube reactor assembly as shown in Figure 5. The quartz tube extends beyond the limits of the concentrated solar flux provided by the HFSF. The quartz tube was positioned at the nominal focus along the optical axis of the HFSF with its axis "vertical".

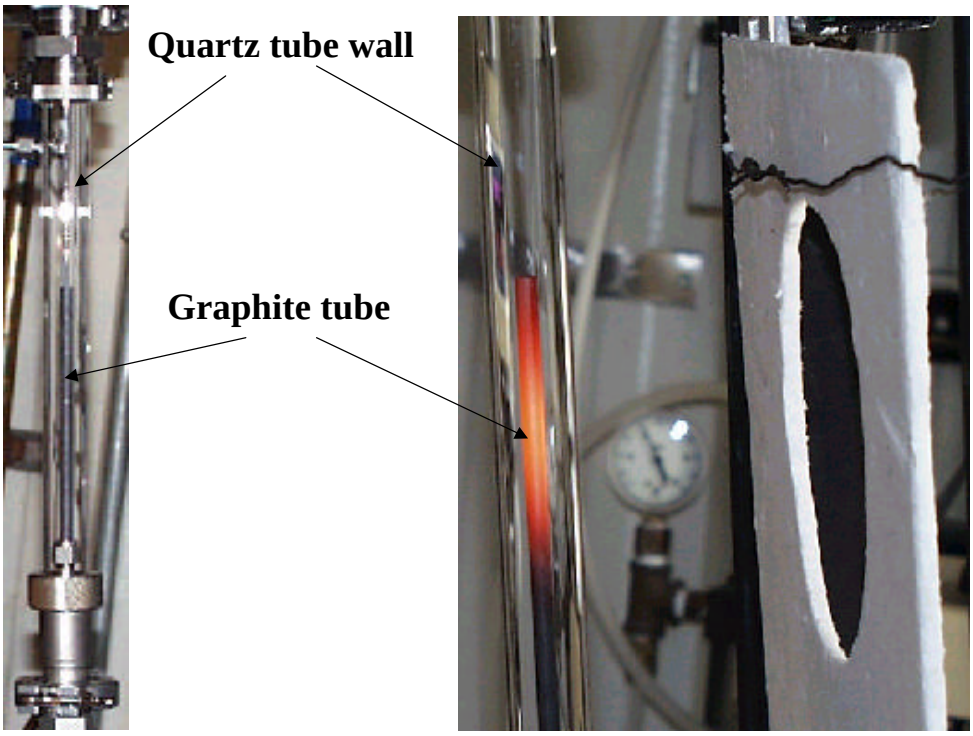

Figure 5. Reactor Tube Assembly: a. before heating, b. immediately after heating (shutter closed)

The particle suspension is generated in a feed mechanism located below the quartz tube (see Figure 6). Lightly compacted carbon black particles ("Shawinigan^{TM}" acetylene carbon black; product of Chevron Chemical Co., Houston, TX) are fed against a rotating steel brush that conveys the particles to a space where they are mixed with the 5% CH_4/Ar feed gas. The suspension then flows through a set of nozzles that destroy any particle agglomerates. The nozzle size varies between 0.33 mm and 0.64 mm. Before the particle cloud passes through the focal area, two streams of "sweep" Ar gas are "wrapped" around the gas-solid suspension. This "fluid-wall" is designed to prevent particles from reaching the quartz glass in locations where heating by the highly concentrated sunlight might soften or melt the tube. The gas and particles are fed from bottom to top of the quartz reactor. With the ratio of "sweep" Ar to feed 5% CH_4/Ar on the order of 10:1, the overall percentage of CH_4 or H_2 was relatively low for these proof-of-concept experiments. These low concentrations are used as a safety precaution for initial studies. A side view of the reactor assembly above the particle feeding system is shown in Figure 7.

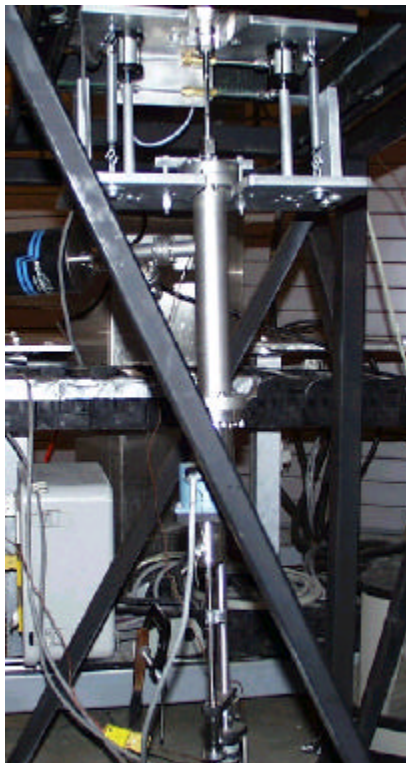

Figure 6. Particle Feeding System (below reactor assembly)

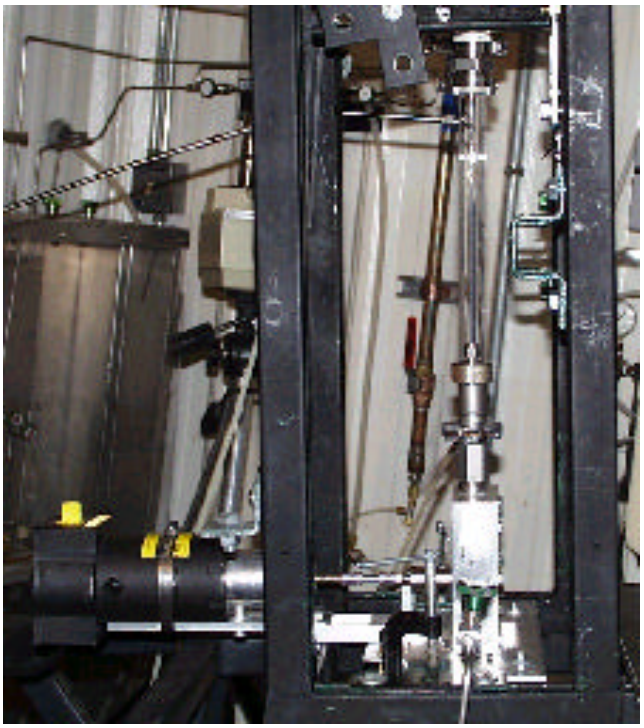

Figure 7. Reactor Assembly (above particle feeding system)

Proof-of-concept Results and Discussion

The signal response for a typical experiment is shown in Figure 8. This was a very clear day with direct normal irradiance at approximately 1000 W/m^2. The estimated flux on the target (reactor) was about 2400 kW/m^2 or 2400 suns. The gas temperature was monitored by a thermocouple downstream of the reactor and the quartz temperature was monitored with an infrared video camera (IR in Figure 8). First the flow of sweep argon gas was initiated at 2 slpm (standard liters per minute), then the particle feed and 5 mol % CH_4/Ar (at a flow of 0.1 slpm) were started at about 4 minutes (0.22 mol % CH_4/Ar total). The particles and CH_4/Ar feed gas mixture entered the reaction tube through a 0.15-m long internal graphite tube as described earlier. A change in the H_2 % can be seen since the thermal conductivity of CH_4 is higher than argon (there is a time delay for the flow to reach the H_2 detector of about 20 to 30 seconds). This signal was allowed to steady, then the concentrated sunlight was introduced by opening a fast-acting shutter. A nearly immediate increase in the H_2 signal can be seen in the dashed trace. The shutter was closed at about 11 minutes and a corresponding decrease in the H_2 signal can be seen. At 16 minutes the flow of CH_4/Ar feed gas was stopped, then restarted, stopped again and restarted at 0.2 slpm at 18 minutes (0.45 mol % CH_4/Ar total). The changes in the H_2 signal clearly indicate that the H_2 production is following these flow manipulations. A sample bag was filled for subsequent analysis from about 20 to 25 minutes. The shutter was closed at about 27 minutes. The subsequent off-line GC analysis (0.8 mol % H_2, 180 ppm CH_4, 180 ppm C_2H_2, 520 ppm C_2H_4, 0.06 mol % CO, 0.05 mol % CO_2, 1.5 mol % air, balance Ar) of the collected gas sample indicated an 88 % dissociation of methane. The air was introduced when the sample bag was detached from the collection valve and possibly also when attaching it to the GC system. The CO and CO_2 indicate that there is some air in the system. The ethylene and acetylene are incomplete reaction products. At the flows of CH_4 and Ar in this experiment, complete dissociation of CH_4 to H_2 would have yielded 0.91 mol % H_2. These results indicate that, with constant solar flux, an increase in the CH_4 feed rate results in an increase in the H_2 synthesis rate.

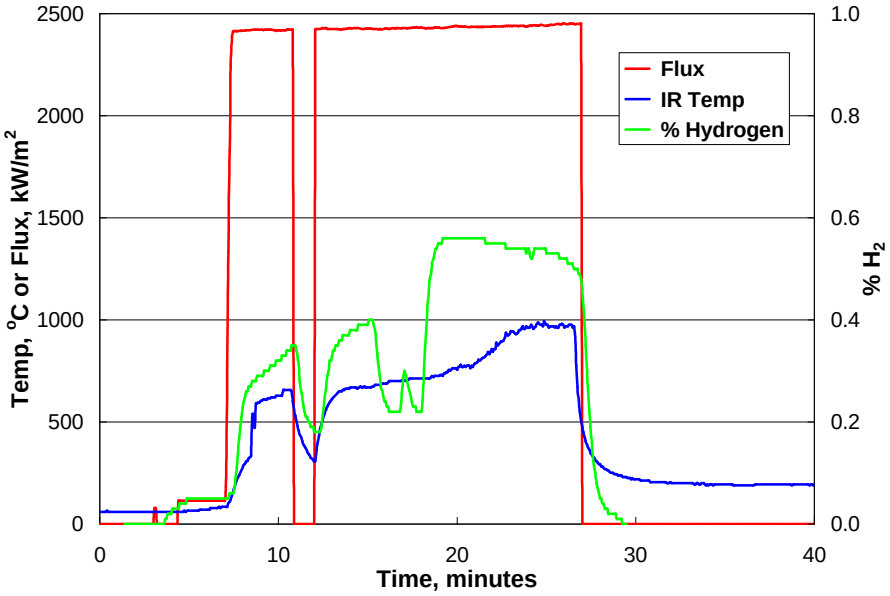

Figure 8. Signal Response to Solar Flux (with particle feed)

Successful experiments were also carried out (Figure 9) without carbon particle co-feed and with a higher concentration of CH_4 in the gas stream (1.7 mol% CH_4/Ar total). When the amount of solar flux striking the reactor increased, the signal from the H_2 detector increased accordingly. In Figure 9, the initial solar flux was 1160 kW/m^2, resulting in little dissociation of CH_4. When the flux was raised to 1760 kW/m^2 the % H_2 signal quickly jumped to over 1 mol % H_2 (about 32% dissociation). As the solar flux continued to increase to 2060 kW/m^2 and 2360 kW/m^2, the H_2 signal increased accordingly to values of 1.4 and 1.5 mol %, respectively. These results indicate that, for a constant CH_4 feed rate, an increase in solar flux results in an increase in the H_2 synthesis rate. The effect of solar flux on dissociation is more apparent from the results presented in Figure 10 for a 1 mol % CH_4 in argon total feed composition. Clearly, a flux of at least approximately 1200 kW/m^2 is necessary to dissociate CH_4.

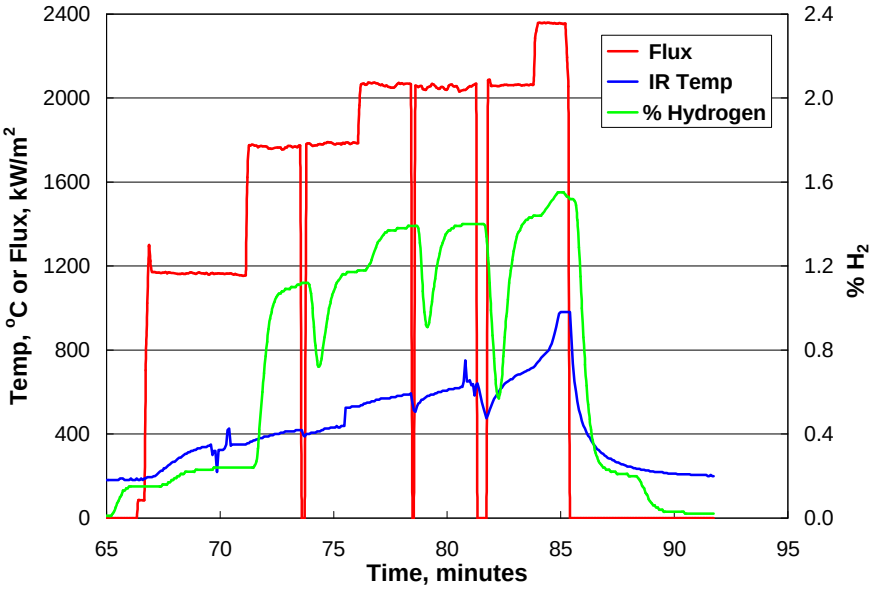

Figure 9. Signal Response to Solar Flux (no particle feed)

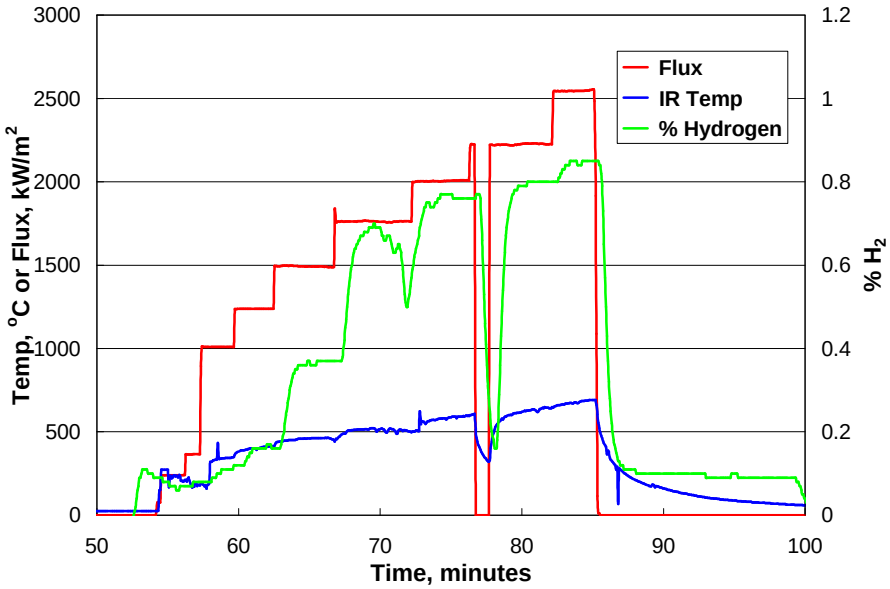

Figure 10. Signal Response to Solar Flux (1 mol % CH_4 in total argon feed)

Process Design and Cost Analysis

A preliminary plant design was developed for a solar-coupled process for the thermal decomposition of methane to hydrogen and carbon black. The process economics were evaluated using discount cash flow analysis. Cash flow analysis determines the required selling prices of the hydrogen and carbon black products. The sales price of these products must generate sufficient revenue to pay for annual operating expenses and the initial capital investment, and provide an acceptable internal rate of return over the lifetime of the process.

Since some of the specific design factors and process costs were not known exactly, these factors and costs were treated as parameters in the analysis. This approach provides insight into how the process economics depends on the values of these factors and costs and determines which factors and costs are most important in determining the overall process economics.

A preliminary evaluation of the current carbon black commercial market was also performed to determine current market sizes for the various grades of carbon black products and their corresponding selling prices. Results from the process design, economic analysis, and market evaluation were used to draw conclusions and make recommendation s for future research and process development.

Process Plant Design

The solar-coupled plant is envisioned to have many of the same unit operations as those of a current commercial carbon black plant [Wang, 1993]. A schematic of the plant is shown in Fig. 11. The reactor is mounted on top of the tower which receives concentrated solar from a field of tracking mirrors or heliostats. The concentrated solar energy provides the energy needs for the process and eliminates the need for partial combustion of the feed. The feed for this process is natural gas, which is preheated in the heat exchanger by the product stream. Natural gas, recycled hydrogen and carbon particles enter the top of the reactor and flow downward where they are heated directly with solar flux. Decomposition of the natural gas results in a product stream consisting of carbon black and hydrogen.

A water quench is not used in this design to maintain a pure stream of carbon black and hydrogen. The product stream flows through the tube side of the heat exchanger and is cooled to about 200^{o}C (473 K) before entering the bag houses. The carbon black is separated in the bag houses and transferred to the storage tanks in the same manner as that of the commercial carbon black process. Hydrogen gas exits the top of the bag houses at near ambient temperature and pressure. A portion of the hydrogen gas is recycled back to the reactor and fed separately to flow past the reactor window and prevent deposition of carbon black. This process design and analysis does not include unit operations for the compression and storage of the hydrogen gas product.

Operation of a solar-coupled plant will be continuous but will only operate when sufficient solar irradiance is available. This fraction of time is referred to as the solar capacity factor and varies with geographic location. Capacity factors for locations that are favorable for solar processes, such as the desert southwest portion of the United States, have been measured to be as high as 0.41. For this work, the capacity factor was varied from 0.28 to 0.41. Limited operation of the

solar-coupled plant results in higher capital costs as compared to a continuous operation plant with the same annual production capacity.

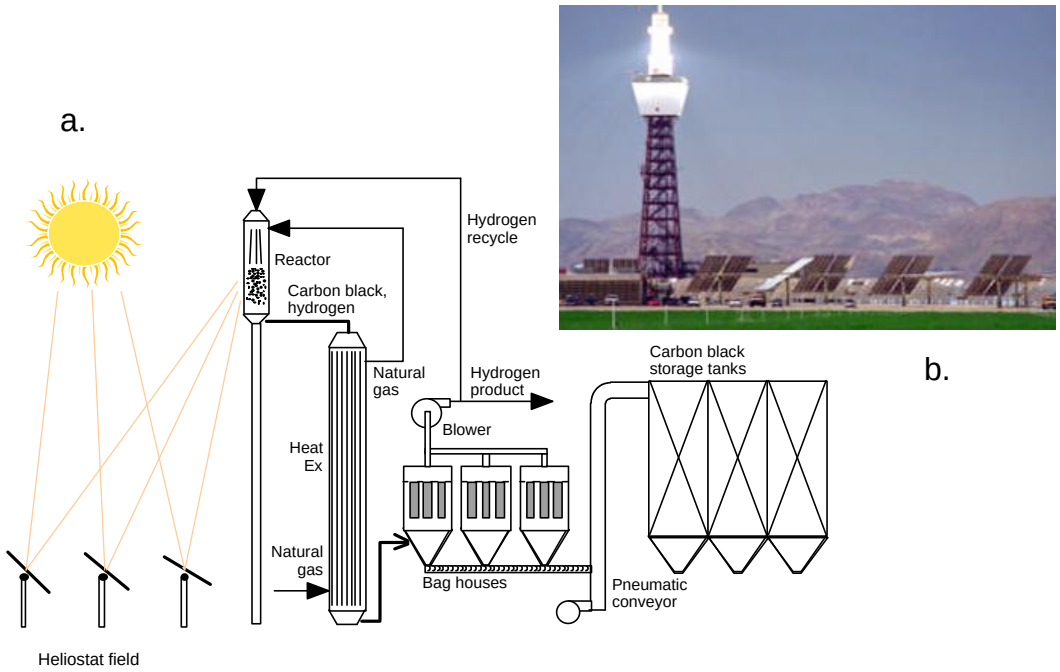

Figure 11. Solar-thermal Processing: a. schematic of aerosol CH_4 dissociation process, b. photograph of 10 MW Barstow, CA facility

Cash Flow Analysis

Cash flow analysis was performed to determine process economics for the solar-coupled process. The analysis consisted of determining the fixed capital and annual operating costs for the process as a function of key design and cost parameters. These parameters included 1) heliostat cost, 2) annual production rate, 3) reaction temperature, 4) reaction residence time, 5) hydrogen fraction recycled, 6) reactor thermal efficiency, and 7) solar capacity factor. The methods for determining these costs are described below.

After fixed capital and annual operating costs for each case were determined, cash flow analysis was performed to determine the required selling prices for hydrogen and carbon black. The cash flow analysis had the following assumptions:

1. Project lifetime: 21 years
2. Construction period: 1 year
3. Working capital: 10% of total capital
4. Capital depreciated, 10% per year
5. Tax rate: 28%
6. Internal rate of return (IRR): 15%

Cash flow analysis determined the required selling prices of hydrogen and carbon black to achieve a net present value of zero at the end of the lifetime of the process. This approach is consistent with the method used by the Hydrogen Program to assess the economics of hydrogen production processes [Mann, 1995]. For all cases, the hydrogen that was produced was assumed to have an energy content of 39.4 kWhr/kg (0.0611 MBtu/lb), which corresponds to its higher heating value (HHV). The final hydrogen product was at ambient temperature and pressure.

Capital Cost Estimation

The capital equipment items for the process included the land, heliostats and tower, reactor, heat exchanger, bag houses, pneumatic conveyor, blower, and storage tanks. For each item, a purchase cost was determined. Methods for calculating purchase costs for each item are described below. The purchase cost included shipping and sales taxes. The fixed capital cost for each item was determined by multiplying the purchase cost by an inflation factor, a set of direct and indirect cost factors, and a contingency and fee. These factors varied with equipment item and values and are summarized in Table 1. For each item, the fixed capital cost was determined by the formula:

$$\text{Fixed Capital Cost} = \text{Purchase cost} * F^{\text{Inflation}} * (1 + F^{\text{Direct}} + F^{\text{Indirect}}) * (1 + F^{\text{Contingency\&Fee}}) \qquad (2)$$

Each item had an inflation factor based on the year from which purchase costs were obtained. All inflation factors were based on cost indices taken from Chemical Engineering (2000). The heliostat, tower, and reactor purchase costs were based on current (2000) cost estimates so the factor for those items was 1. The bag house costs were determined from an estimation procedure based on 1987 costs [Turner et al., 1987a,b]. Purchase costs for the remainder of the equipment items were based on cost tables for January 1990 taken from Peters & Timmerhaus (1991).

The purchase price of land was assumed to be current (Year 2000) at \$500/1000m^2. Since the cost of land improvement was factored into the cost of equipment, all of the direct and indirect cost factors were taken to be 0 for land. For this item, the fixed capital and purchase costs were equal. The quantity of land required for the process was determined from the required heliostat area. The ratio of required land area to heliostat area was 6 to account for reasonable spacing between heliostats.

Table 1. Capital Cost Factors for Purchased Capital Equipment

Factors	Heliostats & Tower	Reactor	Bag Houses	Heat EX, etc
Inflation	1 (2000)	1 (2000)	1.56 (1987)	1.41 (1990)
Direct				
Foundation prep.	0	0	0.1	0.1
Support housing	0	0.08	0	0
Installation	0	0.39	0.39	0.39
Electrical & piping	0	0.41	0.41	0.41
Instrum & controls	0	0.15	0.15	0.15
Service facilities	0.1	0.55	0.55	0.55

Factors	Heliostats & Tower	Reactor	Bag Houses	Heat EX, etc
Indirect				
Engineering	0.1	0.32	0.32	0.32
Construction	0.1	0.34	0.34	0.34
Contingency & fee	0.1	0.15	0.15	0.15

The purchase cost for heliostats and tower were assumed to include most of the direct cost factors listed in Table 1. A cost factor was included for the cost of service facilities. Because the capital expense for these items is much greater than that of the process equipment, the indirect cost factors and contingency & fee were assumed to be less for these items. The tower was assumed to cost $7,500/m of height. This cost is based on estimates from Epstein et al. (1996). The estimated cost for heliostats varies widely depending on the size of the plant and state of maturity of the solar industry. For this reason, heliostat cost was made a parameter in this analysis. Values from $50/m^2 to $1000/m^2 were evaluated. Epstein et al. (1996) reported a vendor heliostat quotation of $150/m^2 (for 60,800 m^2 of heliostat) installed, but not including the foundation, wiring, or site development.

The tower height was determined from the heliostat area according to the formula [Precision Glassblowing, 2000]:

$$\text{Height} = 10*(\text{heliostat area}/1000)^{0.5} \quad (3)$$

This formula accounts for the need to increase the tower height as the heliostat area increases. This is done to prevent shading between heliostats. The heliostat area was determined from the required reactor power, the available solar resource, and several efficiency factors, which account for energy losses as the power is delivered to the reactor. Heliostat area was determined using the expression:

$$\text{Heliostat area} = \text{Power}^{\text{reactor}}/\text{Efficiency}^{\text{reactor}}/\text{Efficiency}^{\text{heliostat}}/\text{Resouce} \quad (4)$$

In this formula, Power$^{\text{reactor}}$ is the required reactor power in kW. Efficiency$^{\text{reactor}}$ is the thermal efficiency of the reactor. It accounts for thermal energy losses through the reactor walls and window. Most of the loss results from radiation losses through the window. This efficiency was evaluated as a parameter with values of 0.3, 0.5, and 0.7. Efficiency$^{\text{heliostat}}$ is the efficiency of the heliostats. It accounts for reflectivity losses (about 5%), projected area losses due to the angle between the incident sunlight and the target reactor and soiling due to dust and dirt. Values for this efficiency vary depending on the location of the heliostat and tower relative to the position of the sun in the sky. An average value for all of the heliostats was assumed to be 0.69. Resource is the average solar resource that is available when the plant is operating. For this analysis, the solar resource was assumed to be 0.75 kW/m^2. Once reactor power is known, values for heliostat area and tower height, along with their corresponding fixed capital costs can be determined from the above formulas.

The reactor was assumed to be a vertical, cylindrical design with some portion or all of the reactor length consisting of a quartz wall that is supported inside a steel housing. A portion of the length would not have the steel housing and would function as the window. A cost factor was included for the steel housing and insulation. There was no cost factor for foundation preparation since the reactor is mounted on top of the tower. The purchase cost was based on cost estimates obtained from a local vender [Precision Glassblowing, 2000] for quartz tubing having diameters of 1, 2, 2.5, 3, and 3.5 ft (i.e. 0.305, 0.61, 0.762, 0.914, and 1.07 m). For all sizes, the cost of the quartz tubing, on a volume basis, varied from $\$900/ft^3$ to $\$1,200/ft^3$ ($\$31,780$ to $\$42,373/m^3$). The purchase cost of the reactor was chosen to be $\$1,100/ft^3$ or $\$38,870/m^3$. The purchase cost of the reactor was assumed to be linear with reactor volume.

The key factors for determining the reactor volume were the volumetric flow rate and reactor residence time. Since the molar and volumetric flow rates increase as the decomposition of methane proceeds, these flow rates were based on product flow rates. Direct heating of the reactants in the reactor is expected to allow for very short residence times. The residence time was evaluated as a parameter with conservative values from 1 to 4 seconds, although fractions of a second have been shown to be sufficient (Figure 2). The total volumetric flow rate depends on the instantaneous molar flow rate of methane, the fraction of recycled hydrogen, and the reactor temperature and pressure. The instantaneous molar flow rate of methane was determined from the annual production of hydrogen, using the solar capacity factor to account for the actual operating time. The total molar flow rate through the reactor assumed that all methane is converted to hydrogen and accounts for the additional molar flow due to recycled hydrogen. The total volumetric flow rate was determined from the total molar flow rate, reactor temperature and pressure, using the ideal gas law as the state function. Reactor pressure was atmospheric for all cases. Reactor temperature was varied as a parameter from 1,600 to 1,900^oC (1873 to 2173 K).

To determine heliostat area, total reactor power was also determined. This was based on the instantaneous molar flow rate of methane, the molar heat of reaction, and the energy required to heat methane to the reaction temperature. Values for the heat of reaction and enthalpy for methane as a function of temperature were obtained from Roine (1997). A portion of the sensible energy in the products is recovered in the heat exchanger. This recovered power is accounted for as a credit in the total reactor power calculation.

A summary of the equipment size and equipment fixed capital cost according to equation (2) for each piece of equipment is included in Table 2 for the base case of 1,000,000 kg H_2/yr. The total equipment fixed capital investment is $7,941,000.

Table 2. Summary of Fixed Capital Equipment Cost (Base Case)

Equipment	Size	Fixed Capital Cost
Land:	72,608 m^2	$36,300
Heliostat:	12,101 m^2	$4,360,000
Tower:	35 m	$376,000
Reactor:	3.13 MWth, 10.4 m^3	$1,513,000
Heat Exchanger:	795 m^2	$620,000

Equipment	Size	Fixed Capital Cost
Baghouse Filter:	117 m^2	$137,000
Other Equipment		Other Equipment Total:
Pneumatic Conveyer:	1000 kg/hr	$936,000
Storage Tanks:	115 m^3	
& Blower:	2.36 m^3/s (5,000 acfm)	
Total Equipment:		$7,941,000

The operating and maintenance (O&M) costs for the process were determined for each major equipment item. The annual cost of natural gas ($594,000/yr @ $3.00/1000 scf) was also determined. For each item, the number of labor hours per day or per some measure of equipment size or production capacity was estimated. This yielded a 7.5 operator/labor force with a fully-burdened labor rate of $40/hour/operator. Supervision labor was estimated at 15% of the total O&M labor.

Base Case

A base case for the process was developed in which the most likely values for the parameters were used. The parameter values for the base case are given in Table 3.

Table 3. Parameter Values for the Base Case

Parameter	Value
Annual hydrogen production	1,000,000 kg/yr
Heliostat cost	$250/$m^2$
Fraction of hydrogen recycled	0.2
Reactor temperature	1,600^{o}C (1873 K)
Reactor residence time	1 second
Reactor thermal efficiency	0.5
Solar capacity factor	0.28

Cash flow analysis determined the required selling prices of hydrogen and carbon black to achieve a net present value of zero at the end of the lifetime of the plant. A graph of the annual and cumulative discount cash flow over the lifetime of the process is shown in Fig. 12.

Various price combinations for hydrogen and carbon black were determined. The extreme cases are hydrogen sales only where the price of carbon black is $0/kg and carbon black sales only where the hydrogen price is $0/kWhr. Intermediate cases set the price for carbon black and the required price for hydrogen was determined. A summary of these results is presented in Table 4.

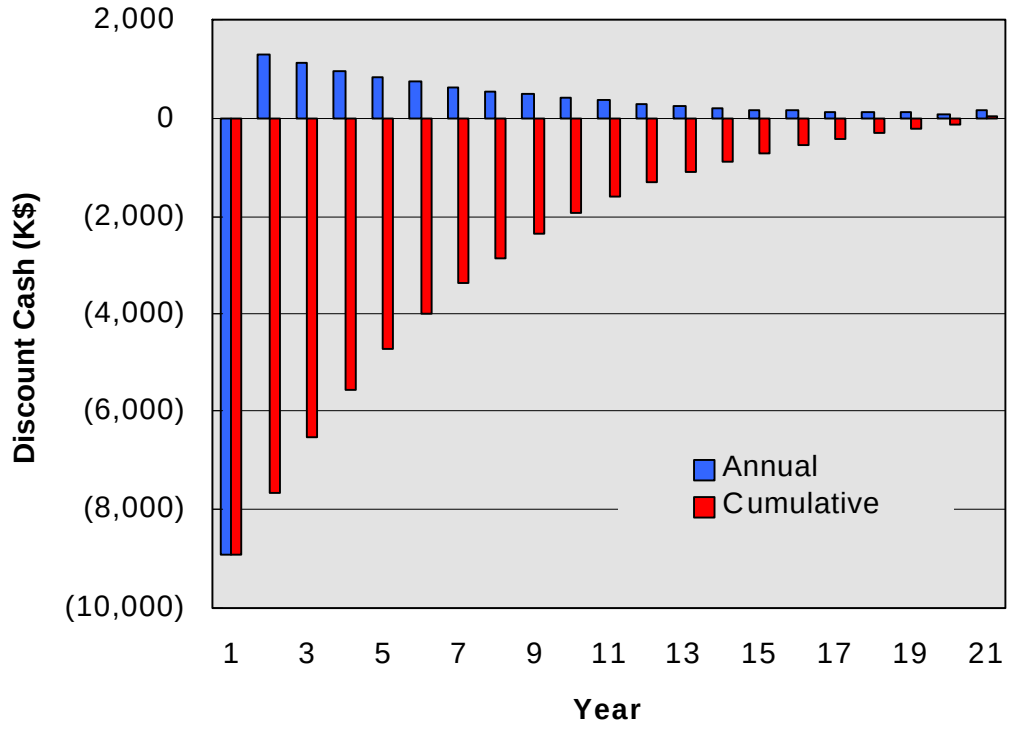

Figure 12. Annual and Cumulative Discount Cash Flow (Base Case)

Table 4. Required Sales Prices for Hydrogen and Carbon Black for Base Case.

Case	Hydrogen Selling Price			Carbon Black Selling Price	
	($/MBtu)	($/kWhr)	($/GJ)	($/lb)	($/kg)
1	27	0.0922	26.2	0.00	0.00
2	20	0.0683	19.0	0.15	0.33
3	15	0.0512	14.2	0.25	0.55
4	10	0.0341	9.5	0.35	0.77
5	5	0.0171	4.8	0.45	0.99
6	0	0	0	0.55	1.21

Results show that if only hydrogen is sold, the price must be $27/MBtu ($0.0922/kWhr or $26.2/GJ). If only carbon black is sold, the price must be $0.55/lb ($1.21/kg).

Another scenario was considered in which the solar capital and operating costs were set to 0 and the hydrogen product was assumed to provide the thermal energy requirements for the process. The hydrogen byproduct in the conventional process is often used in this manner. For this scenario, the hydrogen price would be $0.0/kWhr. Since the process is not solar-coupled, the capacity factor can be increased from 0.28 to 0.95, indicating the plant would operate 95% of the time. The selling price of carbon black was determined using several values for reactor residence

time. In the commercial process, the reactor residence time is typically greater than 1 second. Results are presented in Table 5.

Table 5. Selling Price for Carbon Black vs. Residence Time (conventional plant).

Reactor Residence Time	Carbon Black Price	
(seconds)	($/lb)	($/kg)
1	0.22	0.49
2	0.25	0.55
3	0.27	0.60
4	0.33	0.73

These costs are consistent with the current selling price of commercial carbon black that sells for $0.30/lb to $0.35/lb ($.66/kg to $0.77/kg) [Chemical Marketing Reporter, 2000] and indicate that the economic analysis for the conventional portions of this plant are reasonable.

Parametric Analysis

The selling prices for hydrogen and carbon black were determined for variations of the base case in which the parameter values, which are listed in Table 3, were varied one at a time. The cost of heliostats is uncertain because the technology and the market are still developing. This cost was varied from $50/m^2 to $1000/m^2. Results are presented in Table 6 with prices assuming only one product is sold.

Table 6. Selling Prices for Hydrogen and Carbon Black vs. Heliostat Cost

Heliostat Cost	Hydrogen Selling Price			Carbon Black Selling Price	
($/m^2)	($/MBtu)	($/kWhr)	($/GJ)	($/lb)	($/kg)
50	22	0.0751	20.9	0.44	0.97
100	23	0.0785	21.8	0.47	1.04
250	27	0.0922	25.6	0.55	1.21
500	34	0.1161	32.3	0.70	1.54
750	41	0.1400	38.9	0.84	1.85
1000	48	0.1639	45.5	0.98	2.16

Other parameter values in Table 3 were also varied to determine the variation of selling prices with the values of these parameters. Each of the following parameter variations assumes that only one product is sold. As with the other cost studies in this paper, the required selling price of hydrogen will be reduced if the carbon black can be sold, and vice versa. When the size of the plant was decreased from 1,000,000 kg/yr to 100,000 kg/yr, the required sales price of hydrogen increased to $32/MBtu ($0.1092/kWhr or $30.3/GJ) and the price of carbon black increased to $0.65/lb ($1.43/kg).

A portion of the hydrogen product must be recycled back to the reactor in order to keep the window clean and cool. Increasing the recycled fraction increases the total gas volumetric flow through the reactor and therefore, reactor size and cost. When the fraction of recycled hydrogen increased from 0.2 to 0.5, the sales price of hydrogen increased to $29/MBtu ($0.099/kWhr or $27.5/GJ) and the sales price of carbon black increased to $0.59/lb ($1.30/kg). Increasing the reactor temperature may improve the carbon black product quality. Increasing the reactor temperature also increases total gas volumetric flow through the reactor. When the reactor temperature is increased to 1,900^{o}C (2173 K) the hydrogen price increased to $29/MBtu ($0.099/kWhr or $27.5/GJ) and the carbon black price to $0.58/lb ($1.28/kg). Increasing the reactor residence time may allow for lower operating temperatures but also increases reactor size. Increasing the residence time to 2 seconds increased the hydrogen sales price to $32/MBtu ($0.1092/kWhr or $30.3/GJ) and the carbon black sales price to $0.65/lb ($1.43/kg).

Decreasing the reactor thermal efficiency increases the thermal energy requirement for the reaction, and therefore, the size of the heliostat field. Decreasing this efficiency from 0.5 to 0.25 increased the sales price of hydrogen to $39/MBtu ($0.133/kWhr or $36.9/GJ) and the sales price of carbon black to $0.79/lb ($1.74/kg).

The solar capacity factor will also impact the economics of the process. Values for this factor have been measured to be as high as 0.41 in areas of very high solar irradiance. Increasing the capacity factor from 0.28 to 0.41 decreases the price of hydrogen to $22/MBtu ($0.075/kWhr or $20.8/GJ) and the price of carbon black to $0.44/lb (0.97/kg).

The profitability analysis is summarized in Figure 13. The effect of heliostat cost and reactor efficiency on required hydrogen selling price is shown at arbitrary, fixed values of carbon black selling price.

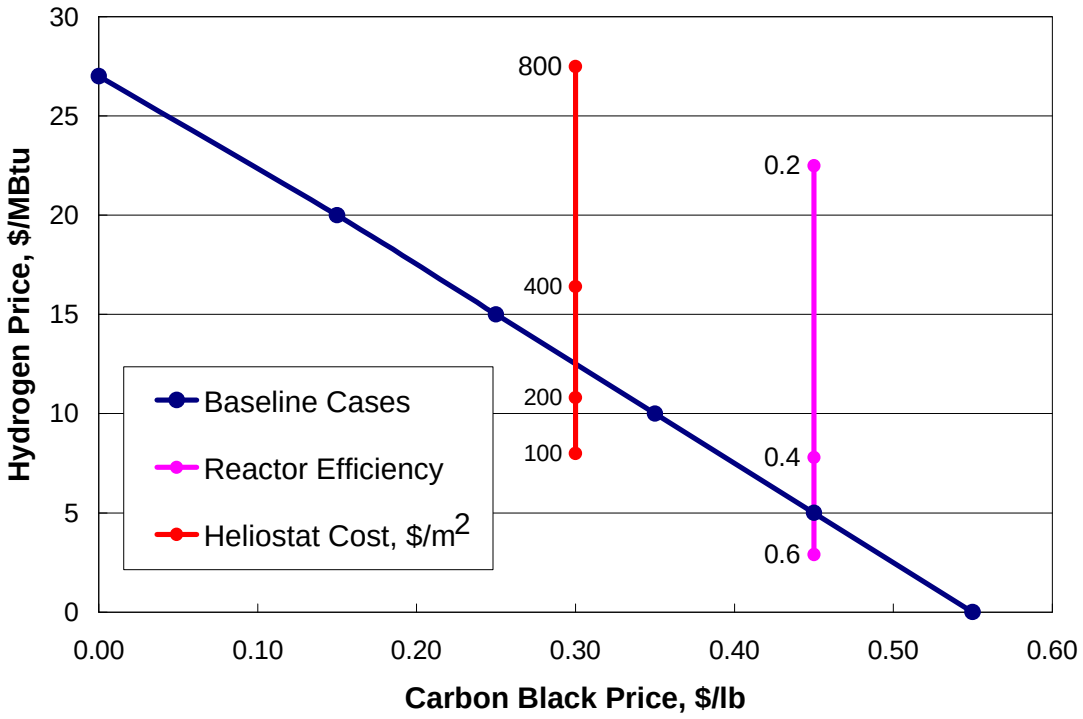

Figure 13. Profitability Analysis Summary

Market Analysis for Carbon Black

A preliminary evaluation of the current carbon black commercial market was also performed to determine current market sizes for the various grades of carbon black products and their corresponding selling prices. Applications for carbon black include the reinforcement of rubber, use as black pigment, and as a conductive additive to rubber and plastic products [Kirk-Othmer, 1991]. World production of carbon black in 1989 was greater than 6 million metric tons. United States production was about 1.6 million metric tons. About 70% of the carbon black that is produced is used in the reinforcement of rubber for tires, 20% is used in other rubber products, and the remaining 10% in non-rubber products. Carbon black used for rubber reinforcement sells for about $0.30/lb to $0.35/lb ($0.66/kg to $0.77/kg) [Chemical Marketing Reporter, 2000].

The non-rubber applications include additives to plastics, printing inks, paint, and paper. A special electrically conductive grade of carbon black sells for prices that are considerably higher than those that are used in rubber reinforcement. Electrically conductive grades are used to produce conductive and antistatic polymer composites. Applications include antistatic carpeting, floor tile, heating elements, videotapes and disks, and electrical shielding. Markets for these applications are increasing faster, on a percentage basis, than those for conventional uses. The current price for a higher grade of carbon black (Thermax) is $0.78/lb [Canadian Carbon Company, 2000]. An even higher grade of carbon black produced from acetylene sells for $1.40/lb [Chevron Chemical Company, 2000].

In 1989, the total market for specialty grade carbon blacks was 126,000 metric tons or 126,000,000 kg. A solar-coupled hydrogen production plant, which produces 1,000,000 kg/yr of hydrogen, will produce 3,000,000 kg/yr of carbon black. This represents about 2.4% of the current United States market for higher-grade carbon blacks. The addition of this production capacity to the current market would not have a significant impact on the price of higher-grade carbon blacks and since this market is increasing faster than other carbon black markets, demand for the additional production capacity should be easy to identify.

Summary and Conclusions

The objectives of this work were to carry out “proof-of-concept” experiments at the NREL HFSF, develop a preliminary design for a solar-coupled process for the thermal decomposition of methane to hydrogen and carbon black, and to evaluate the process economics using discount cash flow analysis. The initial results are encouraging and have demonstrated that the process works in principle. High conversions have been achieved using a solar-thermal reactor not designed for the specific process using only modest solar concentration levels.

The conceptualized plant design includes the same major equipment components as current commercial carbon black production plants. These components include a high temperature reactor, heat exchanger, bag house filters, pneumatic conveyor, blower, and storage tanks. In addition, the process includes a solar heliostat field and tower to provide the thermal energy needs of the process. The process design and economic analysis contain enough refinement to determine how the price of hydrogen and carbon black vary with the values of several key

process parameters and costs. Parametric analysis provides insight into how the process economics depends on the values of these factors and costs and determines which factors and costs are most important in determining the overall process economics.

Results of the discount cash flow analysis show that the required single product selling price for hydrogen for the base case 1,000,000 kg/yr hydrogen plant is $27/MBtu ($0.0922/kWhr or $25.6/GJ) and for carbon black is $0.55/lb ($1.21/kg). These prices assume that only one product is sold. If both products are sold, then the selling price for each decreases. For example, selling prices of $10/MBtu ($0.0341/kWhr or $9.5/GJ) for hydrogen and $0.35/lb ($0.77/kg) for carbon black meet the discounted cash flow requirements. An analysis of the price of carbon black when the solar costs are set to 0 and the hydrogen is used to provide the thermal energy needs of the process indicates that the selling price for carbon black needs to be in the range of $0.22/lb to $0.33/lb ($0.49/kg to $0.73/kg). These results are consistent with the current prices for commercial carbon black.

The selling prices were determined as a function of heliostat costs because the cost of heliostats is uncertain due to a developing technology and market. The heliostat cost was varied from $50/$m^2$ to $1000/$m^2$. The hydrogen price varied from $22/MBtu ($0.075/kWhr or $20.8/GJ) to $48/MBtu ($0.164/kWhr or $45.6/GJ) to while the carbon black price varied from $0.44/lb ($0.97/kg) to $0.98/lb ($2.16/kg). Variation of the prices with other process parameters showed that the prices did not vary dramatically with changes in plant size, hydrogen fraction recycled, reactor temperature and residence time. The prices did increase significantly when the thermal efficiency of the reactor was decreased. This is due to the need for a larger heliostat field as the reactor efficiency decreases.

A preliminary evaluation of the current carbon black commercial market was also performed to determine current market sizes for the various grades of carbon black products and their corresponding selling prices. About 90% of the carbon black that is produced worldwide is used for rubber reinforcement. About 10% is considered specialty grade carbon black and is used as additives in plastics, printing inks, paint, and paper. The current price for a higher grade of carbon blacks is about $0.78/lb ($1.72/kg). A solar-coupled hydrogen production plant, which produces 1,000,000 kg/yr of hydrogen, will produce about 2.4% of the current United States market for higher-grade carbon blacks. Since this market is increasing faster than other carbon black markets, demand for the additional production capacity should be easy to identify.

The encouraging experimental results and attractive economic analysis indicate that this process warrants further investigation. The sensitivity of the hydrogen selling price to reactor efficiency points out the need to focus on reactor design and performance in the next stages of the project.

Acknowledgement

The authors want to thank the DOE Hydrogen Program and The University of Colorado for financially supporting this work under Grants DE-FC36-99GO10454 and DE-PS36-99GO10383.

References

Bromberg, L., D. Cohn, and A. Rabinovich. 1998. "Plasma Reforming of Methane," *Energy & Fuels*, 12, 11-18.

Canadian Carbon Company. 2000. Personal Communication. Cancarb Limited, 1702 Brier Park Crescent NW, Medicine Hat, Alberta, Canada T1A 7G1 (www.CanCarb.com).

Chemical Engineering. 2000. McGraw-Hill Publishing Co. (New York).

Chemical Marketing Reporter. 2000.

Chevron Chemical Company. 2000, Personal Communication, Houston, TX

Donnet, J.B. 1976. Carbon Black, 16-18, Marcel Dekker, New York.

Epstein, M., A. Yogev, I. Hodara, and A. Segal. 1996. "Results of a Feasibility Study on the Possible Use of The Solar Tower Technology at the Dead Sea Works," in *Solar Thermal Concentrating Technologies (Proceedings of the 8th International Symposium, October, 6-11, Koln, Germany (M. Becker and M. Bohmer, editors)*.

Gaudermack, B. and S. Lynum. 1996. "Hydrogen Production from Natural Gas Without Release of CO_2 to the Atmosphere," *Proceedings of the 11th World Hydrogen Energy Conference*, 511-523, Coco Beach, Florida (June, 1996).

Jenkins, D., R. Winston, J. O'Gallagher, C. Bingham, A. Lewandowski, R. Pitts, and K. Scholl. 1996. "Recent Testing of Secondary Concentrators at NREL's High-Flux Solar Furnace," *ASME J. of Solar Energy Engineering*, 29-33.

Kirk-Othmer Encylopedia of Chemical Technologies. 1991. 4th ed., 4, 1037-1072, John Wiley & Sons.

Lee, K.W., W.R. Schofield, and D. Scott Lewis. 1984. "Mobile Reactor Destroys Toxic Wastes *Chemical Engineering*, 46 – 47, April 2, 1984.

Lewandowski, A. 1993. "Deposition of Diamond-Like Carbon Films and Other Materials Processes Using a Solar Furnace," *Mat. Tech*., 8, 237-249.

Lewandowski, A., C. Bingham, J. O'Gallagher, R. Winston, and D. Sagie. 1991. "Performance Characteristics of the SERI High-Flux Solar Furnace," *Solar Energy Materials*, 24, 550-563.

Mann, M.K. 1995. "Technical and Economic Assessment of Producing Hydrogen by Reforming Syngas from the Battelle Indirectly Heated Biomass Gasifier," *NREL/TP-431-8143*, 10-13.

Matovich, E. 1977. "High Temperature Chemical Reaction Processes Utilizing Fluid-Wall *U.S. Patent 4056602* (Nov. 1, 1977).

Mischler, D., R. Pitts, C. Fields, C. Bingham, M. Heben, and A. Lewandowski. 1997. "Solar Production of Fullerenes from a Powdered Graphite Source," *presented at the International Symposium on Solar Chemistry*," Villigen, Switzerland, October 6-7.

Peters, M.S. and K.D. Timmerhaus. 1991. Plant Design & Economics for Chemical Engineers, 4th ed. McGraw-Hill, Inc. (New York).

Pohleny, J.B. and N.H. Scott. 1962. "Method of Hydrogen Production by Catalytic Decomposition of a Gaseous Hydrogen Stream," Chemical Engineering, 69, 90-91.

Pitts, J.R., E. Tracy, Y. Shinton, and C.L. Fields. 1993. "Application of Solar Energy to Surface Modification Processes," *Critical Reviews in Surface Chemistry*, 2 (4), 247.

Roine, A. 1997. *Outokumpu HSC Chemistry for Windows Version 3.0.*

Steinberg, M. 1986. "The Direct Use of Natural Gas for Conversion of Carbonaceous Raw Materials to Fuels and Chemical Feedstocks," *Int. J. Hydrogen Energy*, 11, 715-720.

Steinberg, M. 1987. "A Low Cost High Energy Density Carbon Black Fuel Mix for Heat *Energy Sources*, 9, 161-171.

Steinberg, M. 1994. "Fossil Fuel and Greenhouse Gas Mitigation Technologies," *Int. J. Hydrogen Energy*, 19, 659-665.

Steinberg, M. 1995a. "The Carnol Process for CO_2 Mitigation from Power Plants and the Transportation Sector," *Brookhaven National Laboratory Report BNL 62835*, Upton, NY.

Steinberg, M. 1995b. "The Hy-C Process (Thermal Decomposition of Natural Gas) Potentially the Lowest Cost source of Hydrogen with the Least CO_2 Emission," *Energy Convers. Mgmt.*, 36 (6-9), 791-796.

Steinberg, M. 1998. "Production of Hydrogen and Methanol from Natural Gas with Reduced CO_2 Emission," *Int. J. Hydrogen Energy*, 23, 419-425.

Steinberg, M. 1999. "Fossil Fuel Decarbonization Technology for Mitigating Global Warming," *Int. J. Hydrogen Energy*, 24, 771-777.

Steinberg, M. and H.C. Cheng. 1989. "Modern and Prospective Technologies for Hydrogen Production from Fossil Fuels," *Int. J. Hydrogen Energy*, 14, 797-820.

Turner, J.H., A.S. Viner, J.D. McKenna, R.E. Jenkins, and W.M. Vatavuk. 1987a. "Sizing and Costing of Fabric Filters, Part 1: Sizing Considerations," *JAPCA*, 37 (6), 749-759.

Turner, J.H., A.S. Viner, J.D. McKenna, R.E. Jenkins, and W.M. Vatavuk. 1987b. "Sizing and Costing of Fabric Filters, Part 1: Costing Considerations," *JAPCA*, 37 (9), 1105-1112.

Wang, J. 1993. Carbon Black (2nd ed.), Marcel Dekker.